URSI AP-RASC, Sydney, Australia, 17 – 22 August 2025

Integrated Simultaneous Transmit and Receive Antenna Systems for ISAC Applications

Min Li*(1) and Fanfei Yang(1)
(1) School of Microelectronics, Tianjin University, Tianjin, China; email: min_li@tju.edu.cn

Abstract

This paper presents a novel simultaneous transmit and receive (STAR) antenna system for integrated sensing and communication (ISAC) applications, utilizing the substrate integrated suspended line (SISL) platform to achieve high efficiency and seamless integration. Experimental results show that the STAR antenna provides 40 dB of self-interference cancellation (SIC) within the 4.1–6.7 GHz frequency range while maintaining a stable left-handed circularly polarized (Co-LHCP) radiation pattern for both transmission (TX) and reception (RX). The system supports simultaneous sensing and communication with a bit error rate of less than 0.17% in complex indoor environments, demonstrating its significant potential for multifunctional ISAC applications.

1. Introduction

In the context of fifth-generation advanced (5G-A) and sixth-generation (6G) mobile communications, the escalating scarcity of spectrum resources has underscored the urgent need for more efficient utilization. In-band full-duplex (IBFD), or simultaneous transmit and receive (STAR), has emerged as a promising approach, offering the theoretical potential to double spectral efficiency. Moreover, it facilitates seamless integration with advanced technologies such as multiple-input multiple-output (MIMO) and beamforming, thereby substantially enhancing channel capacity [1], [2].

A fundamental requirement for enabling STAR operation is the effective cancellation of self-interference (SIC) between the receiver (RX) and transmitter (TX). Numerous techniques have been proposed to mitigate SIC at the antenna level, including cross-polarization [3], [4], decoupling networks [5], [6], near-field cancellation [7], [8], and circulators [9]. Among these, co-circularly polarized (Co-CP) full-duplex antennas have garnered significant attention due to their high TX-RX isolation and consistent radiation characteristics. One approach employs circular modes with two sequentially rotating feeding networks to excite dual-polarized radiators; however, limited operating bandwidths remain a key challenge [10], [11], [12]. Furthermore, wideband designs [13] that utilize coaxial cables often suffer from performance degradation, as the antenna and feeding network are designed separately, leading to compromised isolation and reduced overall efficiency.

This paper introduces a novel Co-CP STAR antenna system based on the substrate-integrated suspended line (SISL) platform [14], which consolidates beamforming, interconnecting networks, and the antenna radiator into a single, compact system. The proposed design achieves wideband operation, high integration, and exceptional efficiency, demonstrating substantial potential for multifunctional integrated sensing and communication (ISAC) applications.

2. Antenna System Configuration

The architecture and geometric configuration of the proposed SISL-based STAR antenna system are presented in Fig. 1. As illustrated in Fig. 1(a), the system comprises three primary components: the metasurface antenna and two feeding networks for transmission (TX) and reception (RX). Each beamforming network for TX and RX incorporates a balun and two 90° hybrid couplers, enabling a sequentially rotated feeding mechanism.

The STAR antenna consists of eleven substrate layers (substrates 1–11), with metalization on both sides (G1-G22). The G6 and G16 layers, located on substrates 3 and 8, respectively, along with the topmost G22 layer on substrate 11, are key components, as highlighted in Fig. 1. The RX feeding network spans substrates 1 to 5, while the TX feeding network extends across substrates 6 through 10, with the antenna positioned on substrate 11. The core beamforming and interconnecting networks are integrated into the G6 and G16 layers, with all substrates assembled using rivets. Substrates 3, 8, and 11 are fabricated from Rogers 4350, which has a relative permittivity of 3.66 to minimize losses, while the remaining substrates are made from FR4. Substrates 2, 4, 7, and 9 feature hollowed-out sections that create air cavities for the suspended lines, thereby minimizing circuit insertion loss.

To integrate the two complex feeding networks for RX and TX within the SISL platform, as depicted in Figs. 1(c) and (d), the main circuits for RX and TX are designed on separate layers, specifically the G6 and G16 layers. These networks excite a coupling slot located at the center (G10 layer), which, in turn, drives the wideband metasurface antenna on the topmost G22 layer.

3. Results and Discussion

3.1 Simulation and Measurement Results

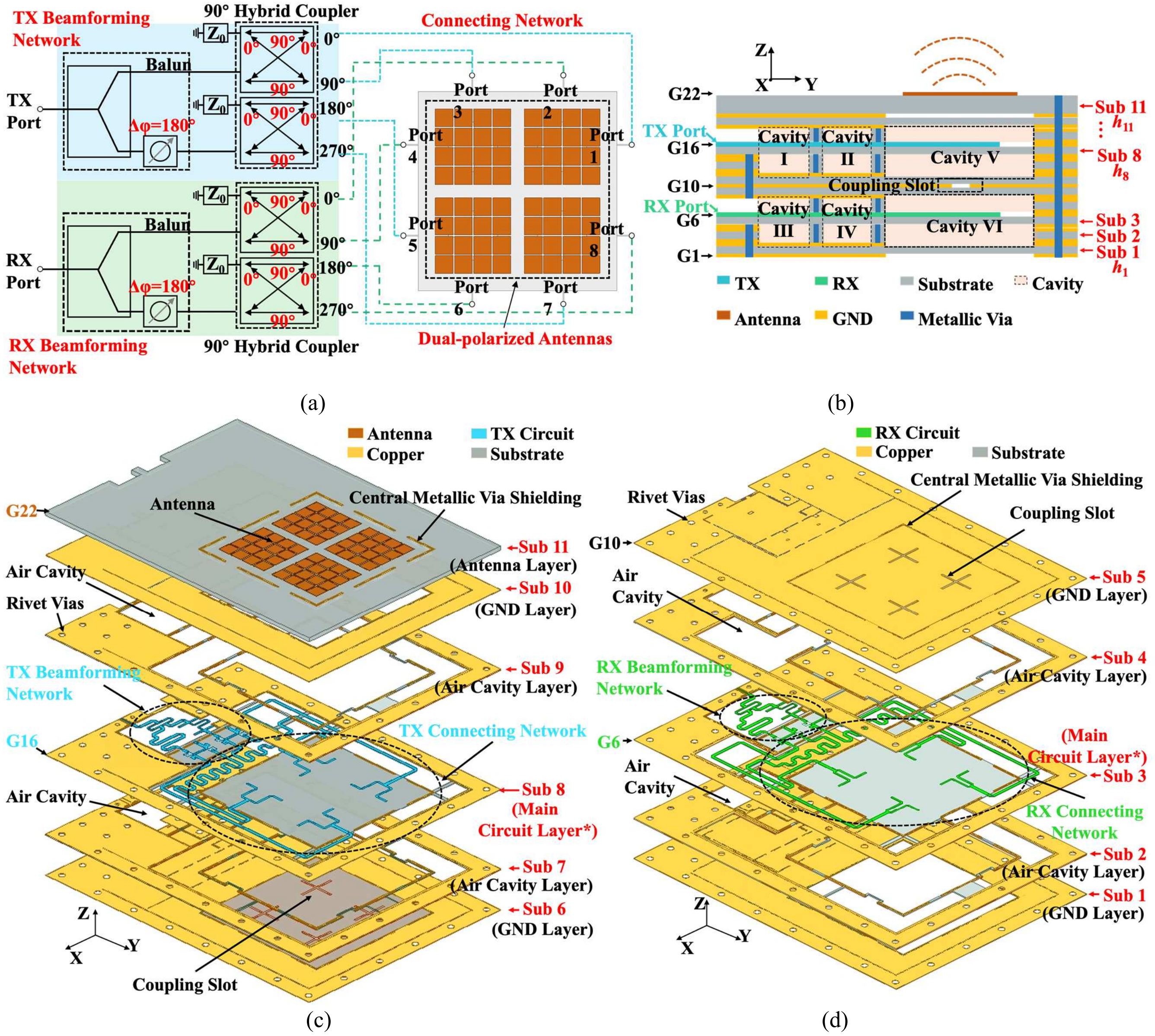

Figure 1. Configuration of the proposed SISL-based STAR antenna system. (a) System architecture diagram. (b) Side view. (c) 3-D view of TX. (d) 3-D view of RX. (h_2=h_4=h_7=h_9=0.5, h_3=h_8=0.2, h_1=h_{10}=0.2, h_5= h_6=0.127, and h_{11}= 2.0. Unit: mm.)

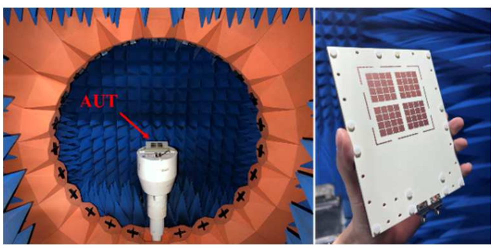

Figure 2. Prototype of the STAR antenna.

A prototype of the SISL STAR antenna, fabricated using low-cost commercial PCB technology, is shown in Fig. 2. The measured reflection coefficients (|S11| and |S22|) in Fig. 3(a) remain below -10 dB over 4.1-6.7 GHz, providing a 48.1% fractional bandwidth, with over 40 dB isolation between TX and RX, as shown in Fig. 3(b). The Co-LHCP

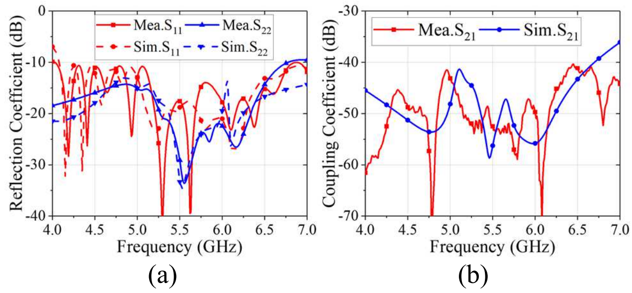

Figure 3. Simulation and measurement results. (a) Reflection coefficients. (b) Coupling coefficients.

radiation patterns for TX and RX, presented in Fig. 4, are nearly identical. The measured axial ratio in Fig. 5 remains within 3 dB over the 3 dB beamwidth. Fig. 6 shows that the total efficiency exceeds 70% from 5.0 to 6.5 GHz, with a peak simulated efficiency of 82% at 5.5 GHz.

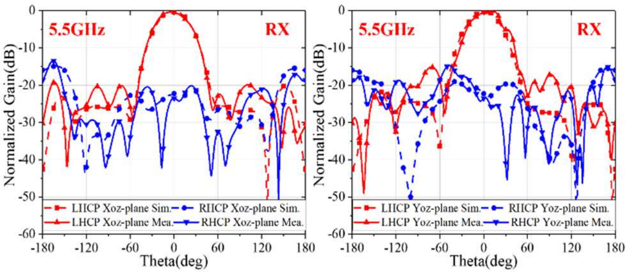

(a)

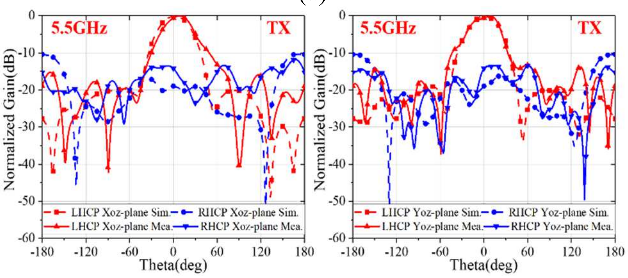

(b)

Figure 4. Simulated and measured radiation patterns of the proposed STAR antenna. (a) RX. (b) TX.

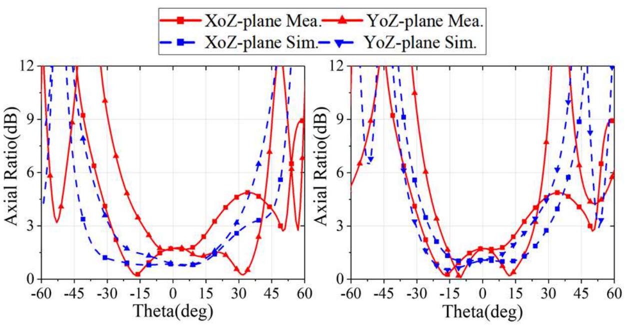

Figure 5. Simulated and measured axial ratio (AR) of the proposed STAR antenna at 5.5 GHz. (a) RX. (b) TX.

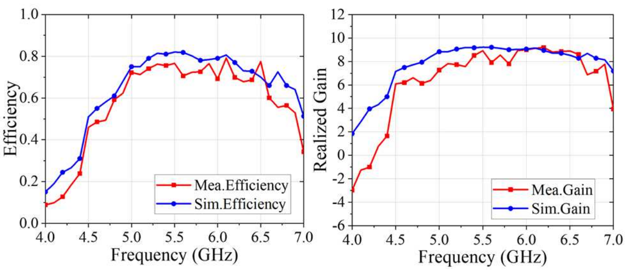

Figure 6. Simulated and measured results. (a) Total efficiency. (b) Realized gain.

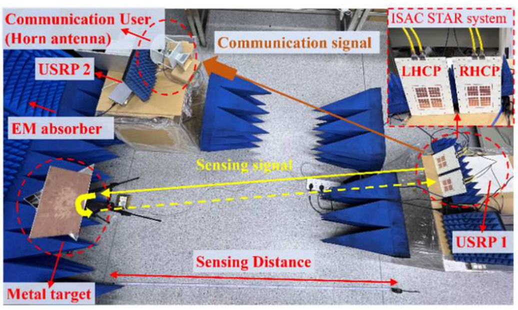

Figure 7. ISAC test environment.

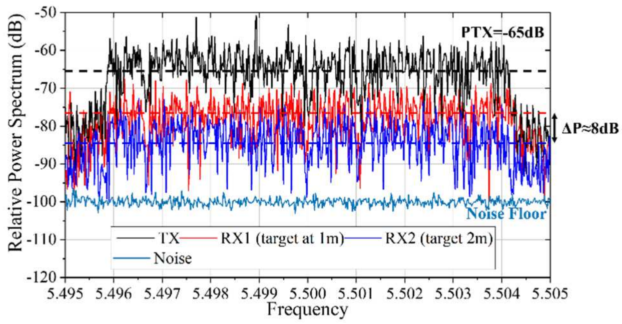

Figure 8. Sensing results showing relative power spectrograms of the proposed ISAC system.

(a) (b)

Figure 9. Communication results of image transfer. (a) Original image. (b) Image with 0.17% BER.

3.2 ISAC Applications

The ISAC test environment, depicted in Fig. 7, is established in a 3×3 m indoor space, equipped with the necessary test instruments, the antenna under evaluation, and absorptive materials. The TX section consists of a processor, a TX universal software radio peripheral (USRP), and the proposed STAR antenna. The USRP generates and modulates the TX signal into an orthogonal frequency division multiplexing (OFDM) waveform, which is then transmitted through the left-handed circular polarized (LHCP) STAR antenna's TX channel.

The communication RX section comprises a horn antenna, an RX USRP, and a processor. The horn antenna receives the communication signal, which is demodulated by the RX USRP and displayed on the processor. The sensing RX section includes the right-handed circular polarized (RHCP) STAR antenna, an RX USRP, and a processor. The RX channel captures the echo signals reflected from a planar metal target after transmission. By analyzing the amplitude and delay of the echo signals, the sensing functionality is achieved.

Fig. 8 shows the TX and RX relative power spectrum of the sensing signal. The TX signal exhibits a relative power of -65 dB. When the target is positioned 1 or 2 meters in front of the ISAC system, the echo signal displays a power difference of approximately 8 dB, with the relative background noise around -100 dB in the indoor environment, confirming effective target detection.

Fig. 9 illustrates the communication performance of the ISAC system. In Fig. 9(a), the original image to be transmitted, with a size of 28,080 bytes, is shown. When the receiving antenna is positioned 2.5 meters from the ISAC transmitter, the received image in Fig. 9(b) exhibits a bit error rate (BER) of 0.17% and slight pixel distortion in the lower-right corner. This is attributed to multipath effects within the complex indoor environment and the limitations of the TX power.

4. Conclusion

This paper presented a novel integrated STAR antenna, developed on the SISL platform, which featured wideband SIC and high overall efficiency. Prototypes of the STAR antenna were fabricated and tested, with both simulated and measured results demonstrating a 40 dB isolation bandwidth from 4.1 to 6.7 GHz (48.1% bandwidth), peak efficiencies exceeding 80%, and stable Co-LHCP RX and TX radiation patterns across the entire frequency range. The system also achieved good communication performance (with a BER of approximately 0.17% at 2.5 m) and effective sensing capabilities. The proposed STAR system successfully integrated communication and sensing functions, confirming its suitability for ISAC applications.

5. Acknowledgements

This work was supported in part by the National Natural Science Foundation of China under Grant 62471332.

References

[1] A. Sabharwal, P. Schniter, D. Guo, D. W. Bliss, S. Rangarajan and R. Wichman, "In-Band Full-Duplex Wireless: Challenges and Opportunities," *IEEE Journal on Selected Areas in Communications*, vol. 32, no. 9, pp. 1637-1652, Sept. 2014.

[2] X. Xia, K. Xu, D. Zhang, Y. Xu and Y. Wang, "Beam-Domain Full-Duplex Massive MIMO: Realizing Co-time Co-frequency Uplink and Downlink Transmission in the Cellular System," *IEEE Transactions on Vehicular Technology*, vol. 66, no. 10, pp. 8845-8862, Oct. 2017.

[3] K. Park, J. Myeong, G. M. Rebeiz and B. -W. Min, "A 28-GHz Full-Duplex Phased Array Front-End Using Two Cross-Polarized Arrays and a Canceller," *IEEE Transactions on Microwave Theory and Techniques*, vol. 69, no. 1, pp. 1127-1135, Jan. 2021.

[4] K. -R. Xiang, F. -C. Chen, Y. -Z. Liang and Q. -X. Chu, "Dual-Polarized Cavity-Backed Full Metal Antennas for In-Band Full-Duplex Application," *IEEE Transactions on Antennas and Propagation*, vol. 71, no. 12, pp. 9375-9385.

[5] L. Ma, J. Lai, Y. Yin, C. Xia, C. Gu and J. Mao, "A Wideband Co-Linearly Polarized Full-Duplex Antenna-in-Package With High Isolation for Integrated Sensing and Communication," *IEEE Antennas and Wireless Propagation Letters*, vol. 22, no. 9, pp. 2185-2189, Sept. 2023.

[6] S. N. Venkatasubramanian, L. Li, A. Lehtovuori, C. Icheln and K. Haneda, "Impact of Using Resistive Elements for Wideband Isolation Improvement," *IEEE Transactions on Antennas and Propagation*, vol. 65, no. 1, pp. 52-62, Jan. 2017.

[7] D. Wu et al., "Wideband Monostatic Co-Horizontally Polarized Simultaneous Transmit and Receive Antenna Subsystem With Integrated Beamforming Network," *IEEE Transactions on Antennas and Propagation*, vol. 70, no. 2, pp. 1505-1510, Feb. 2022.

[8] K. Park, J. Myeong, G. M. Rebeiz and B. -W. Min, "A 28-GHz Full-Duplex Phased Array Front-End Using Two Cross-Polarized Arrays and a Canceller," *IEEE Transactions on Microwave Theory and Techniques*, vol. 69, no. 1, pp. 1127-1135, Jan. 2021.

[9] H. Nawaz and I. Tekin, "Dual-Polarized, Differential Fed Microstrip Patch Antennas With Very High Interport Isolation for Full-Duplex Communication," *IEEE Transactions on Antennas and Propagation*, vol. 65, no. 12, pp. 7355-7360, Dec. 2017.

[10] Z. Zhou, Y. Li, J. Hu, Y. He, Z. Zhang and P. -Y. Chen, "Monostatic Copolarized Simultaneous Transmit and Receive (STAR) Antenna by Integrated Single-Layer Design," *IEEE Antennas and Wireless Propagation Letters*, vol. 18, no. 3, pp. 472-476, March 2019.

[11] J. Ha, M. A. Elmansouri, P. Valale Prasannakumar and D. S. Filipovic, "Monostatic Co-Polarized Full-Duplex Antenna With Left- or Right-Hand Circular Polarization," *IEEE Transactions on Antennas and Propagation*, vol. 65, no. 10, pp. 5103-5111, Oct. 2017.

[12] D. Wu, Y. -X. Sun, B. Wang and R. Lian, "A Compact, Monostatic, Co-Circularly Polarized Simultaneous Transmit and Receive (STAR) Antenna With High Isolation," *IEEE Antennas and Wireless Propagation Letters*, vol. 19, no. 7, pp. 1127-1131, July 2020.

[13] D. Wu, Y. -X. Sun, R. Lian, B. Xiao, M. Li and K. -D. Xu, "Metasurface Antenna With Cocircularly Polarized Radiation Characteristics for Wideband Monostatic Simultaneous Transmit and Receive Applications," *IEEE Transactions on Antennas and Propagation*, vol. 71, no. 4, pp. 3304-3313, April 2023.

[14] K. Ma, N. Yan, and Y. Wang, "Recent progress in SISL circuits and systems: review of passive and active circuits demonstrating SISL's low loss and self-packaging and showcasing the merits of metallic, shielded, suspended lines," *IEEE Microwave Magazine*, vol. 22, no. 4, pp. 49-71, Apr 2021.